THE JOURNAL OF PHYSICAL CHEMISTRY C

Subscriber access provided by CZECH ACADEMY OF SCIENCES

C: Surfaces, Interfaces, Porous Materials, and Catalysis

Catalyst-Free Hydrogen Synthesis from Liquid Ethanol: an ab initio Molecular Dynamics Study

Giuseppe Cassone, Adriano Sofia, Giovanni Rinaldi, and Jiri Sponer

J. Phys. Chem. C, **Just Accepted Manuscript** • DOI: 10.1021/acs.jpcc.9b01037 • Publication Date (Web): 12 Mar 2019

Catalyst-Free Hydrogen Synthesis From Liquid Ethanol: an *ab initio* Molecular Dynamics Study

Giuseppe Cassone*[1ab], Adriano Sofia[2], Giovanni Rinaldi[3], Jiri Sponer[1]

[1] *Institute of Biophysics of the Czech Academy of Sciences, Královopolská 135, 61265 Brno, Czech Republic*

[2] *Università degli Studi di Messina, Dipartimento di Scienze Matematiche e Informatiche, Scienze Fisiche e Scienze della Terra, Contrada Papardo, 98166 Messina, Italy*

[3] *Renewable Energy Group, College of Engineering, Mathematics and Physical Science, University of Exeter, Cornwall Campus, Penryn TR10 9EZ, UK*

(Dated: March 11, 2019)

[a] Email: cassone@ibp.cz

[b] Phone: +420-737963679

ABSTRACT

Hydrogen is the simplest, oldest, and most widespread molecule in Nature. Nevertheless, the vast majority of the hydrogen industrial production stems from steam reforming of methane performed at high temperatures or pressures. Albeit other chemical routes to the hydrogen synthesis – involving, *e.g.*, water electrolysis and novel photocatalysts – have recently been explored, no catalyst-free reaction pathways have been identified, seriously limiting the large-scale deployment of hydrogen. Based on state-of-the-art *ab initio* molecular dynamics simulations, here we present a study revealing a novel synthesis route to hydrogen from neat liquid ethanol, which has been achieved at room temperature and in absence of any catalyst, upon electric field exposure. This result paves the way to the unprecedented catalyst-free experimental synthesis of hydrogen from liquid ethanol by exploiting commonly employed field emitter tips *apparatus*.

I. INTRODUCTION

Hydrogen (H_2) production is estimated to be tenths of millions of tons per year[1,2]. Exploitation of hydrogen ranges from the ammonia production through the Haber-Bosch process[3] to the transport and the conversion of clean energy[4–6]. However, H_2 is always produced by means of specific, costly and rare catalysts. Here we present the first, to the best of our knowledge, catalyst-free chemical route toward the H_2 synthesis.

Although steam reforming of hydrocarbons allows for reasonable hydrogen yields, it produces CO_2 and the reactors typically operate at high temperatures (*i.e.*, $1000-1400$ K) and in presence of specific catalysts[7,8]. The last few decades have witnessed enormous efforts devoted to the design of novel synthesis routes toward the hydrogen production. Many of them involves electrochemical water splitting achieved *via* platinum (Pt) electrocatalysts[9,10] or particulate photocatalysts[11–16]. Recently, metal-free polymeric photocatalysts have been developed[17] and also catalysts of biomolecular nature have been presented[18] as well as prototypical low-cost photoelectrodes[19]. Also simple alcohols are currently employed in steam reforming processes. Being a clean, renewable and reliable chemical carrier of hydrogen, less hazardous than methanol and producible from a wide variety of biomass sources[20], ethanol is considered a promising – fully "green" – alternative. As a consequence, also the catalytic properties of Au loaded into TiO_2 have been characterized for ethanol de-hydrogenation[21].

Whilst many experiments exploited the catalytic electric field assistance in enhancing selectivity of diverse chemical reactions[22–24], the first experimental evidence that intense (*i.e.*, ~ 0.1 V/Å) static fields can fully control chemical transformations has only recently been provided[25]. It seems increasingly evident that oriented electric fields in the order of 1 V/Å will be employed as smart reagents[26] and as catalysts[27] in an imminent future. In particular, nowadays is very well-established by a plethora of experimental, theoretical, and computational works that very intense (*i.e.*, in the order of $0.1-1.0$ V/Å) electric fields rule the microscopic behavior of matter. In addition, many laboratories have become capable to probe and hence quantify the high reactivity-enhancing properties of intense field strengths generated in proximity of emitter tips[25,27,28]. As an example, the experiment that reported the electrostatic catalysis of a Diels-Alder reaction demonstrated that the typical electric field strengths necessary for such a catalysis are in the order of 0.1 V/Å[25]. After all, it has been a long time since a substantial amount of research (see, *e.g.*, Refs.[29–35]) has demon-

strated that intense electric fields (*i.e.*, $\sim [0.1-1.0]$ V/Å) are not only widespread in Nature but also that have to be employed in order to trigger, drive, and/or catalyze, both gas- and condensed-phase chemical reactions. In fact, such field strengths are necessary in order to significantly shift the bonding electrons and render more ionic both bonds and transition states[26]. Thanks to developments of the Modern Theory of Polarization[36,37], nowadays *ab initio* molecular dynamics (AIMD)[29–31,38] and Density Functional Theory-based[32–34] studies have succeeded in describing complex behavior of molecular systems under strong electric fields, quantitatively confirmed by experiments[25,39–42], consolidating those first-principles numerical techniques as robust predictors of laboratory experimental results. The application of electric fields in Density Functional Theory-based simulations allows for the investigation of the reactivity-enhancing properties without the necessity to simulate an entire electrode surface, as already reported in several computational studies (see, *e.g.*, Refs.[29–34]).

II. METHODS

We used the software package Quantum ESPRESSO[43], based on the Car-Parrinello (CP) approach[44], to perform *ab initio* molecular dynamics (AIMD) simulations of a sample of liquid ethanol and a sample composed by an ethanol-water mixture under the action of intense electric fields applied along a given direction (corresponding to the z-axis). The implementation of an external field in numerical codes based on Density Functional Theory (DFT) can be achieved by exploiting the Modern Theory of Polarization and Berry's phases[36,37,45] (see, *e.g.*, Ref.[38]). Thanks to those seminal works, nowadays AIMD simulations under the effect of static electric fields with periodic boundary conditions are almost routinely carried out (see, *e.g.*, Ref[31]). The reader which is interested in the implementation of static electric fields in such a kind of atomistic simulations can refer to the following literature: Refs.[36–38,46–50]. The neat ethanol sample contained 32 CH_3CH_2OH molecules (*i.e.*, 288 atoms) arranged in a cubic cell with side parameter $a = 14.60$ Å, so as to reproduce the experimental density of 0.79 g/cm^3 at about 300 K. The sample simulating the ethanol aqueous solution contained 24 CH_3CH_2OH and 24 H_2O molecules accounting for 288 atoms arranged in a cubic cell with side parameter $a = 14.60$ Å; in such a case a density of 0.82 g/cm^3 has been reproduced. Tests at higher temperatures (*i.e.*, 500 K and 800 K) have been also executed. As usual, the structures were replicated in space by using periodic boundary conditions. The inten-

sity of the electric field was gradually increased with a step increment of about 0.05 V/Å from zero up to a maximum of 0.60 V/Å. In the zero-field cases we performed dynamics of 30 ps whereas, for each other value of the field intensity, we ran the dynamics for 7 ps, thus cumulating a total simulation time equal to 114 ps for each investigated sample. The fictitious electronic mass was set to a value of 300 a.u., with a cutoff energy of 35 Ry for the plane-wave representation of wavefunctions and of 280 Ry for the charge density, with a timestep of 0.12 fs. With such cutoff values the sample is robustly described since the core electronic interaction is being depicted through ultrasoft pseudopotentials (USPP) generated *via* the Rappe-Rabe-Kaxiras-Joannopoulos (RRKJ) method[51]. As an approximation of the exchange and correlation functional, we adopted the Perdew-Burke-Ernzerhof (PBE) functional[52] with Grimme's D3 dispersion corrections[53]. In principle, nuclear quantum effects (NQEs) might play a role in ruling the chemistry of the simulated samples. However, there exist some clear evidences that the inclusion of NQEs in typical AIMD simulations exploiting commonly used dispersion-corrected exchange-correlation functionals – such as PBE-D3 – and which aim at exploring the liquid water behavior do not properly work[54]. Somehow paradoxically indeed not including those NQEs almost perfectly reproduces all the experimental water vibrational modes[54]. This is due to the fact that standard dispersion-corrected exchange-correlation functionals, such as PBE-D3, benefit from error compensation effects that render the NQEs inclusion counter-productive[54]. Moreover, the results we obtained at higher temperatures (*i.e.*, at 500 K and 800 K, where NQEs should be fully negligible) were in complete agreement with the chemistry emerging at room temperature. As a consequence, the dynamics of ions was simulated classically within a constant number, volume, and temperature (NVT) ensemble, using the Verlet algorithm and a Nosé-Hoover thermostat set at a frequency of 13.5 THz.

III. RESULTS AND DISCUSSION

Since the application of weak electric fields reduces the activation energies for ethanol de-hydrogenation in presence of Pt-based catalysts[55], we decided to apply progressively increasing field strengths to samples of neat ethanol and ethanol-water mixtures. Upon exposure of a sample of pure liquid ethanol to progressively higher field intensities, increasingly larger fractions of the OH alcohol groups tend to align toward the field direction, as

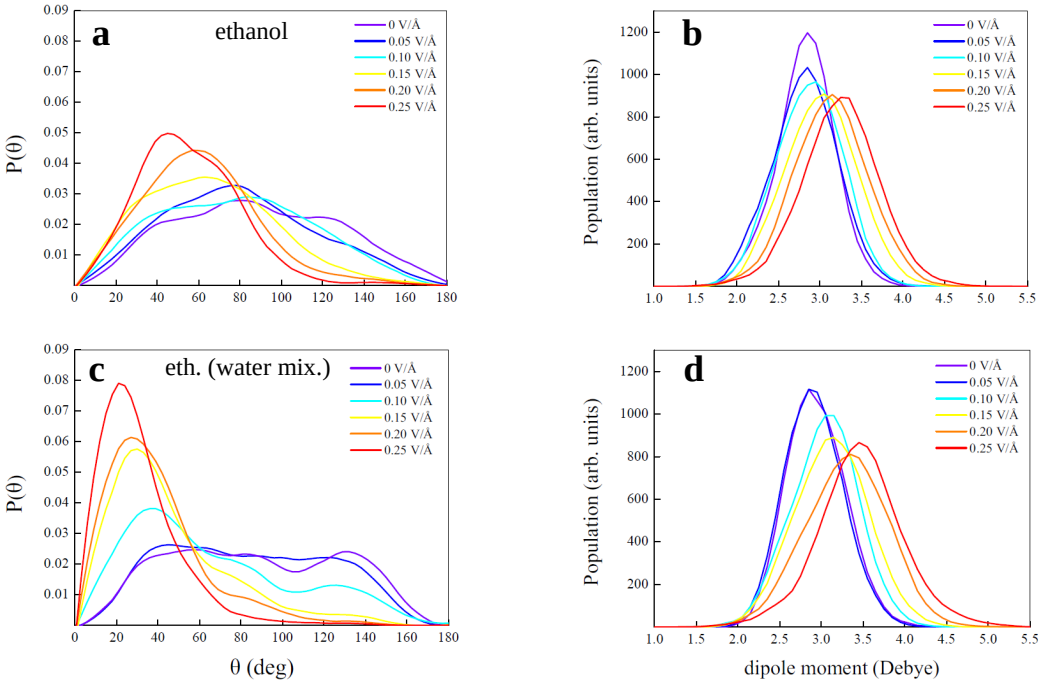

FIG. 1: (a/c) Distributions of the θ angle formed between the vector identifying the O-H bonds of the ethanol molecules and the field direction in neat ethanol (a) and in an ethanol-water mixture (c) from the zero-field regime (purple curve) up to 0.25 V/Å (red curve). (b/d) Dipole moments distribution functions of the ethanol molecules in neat ethanol (b) and in an ethanol aqueous solution (d) from the zero-field regime (purple curve) up to 0.25 V/Å (red curve).

shown in Fig. 1-a. At the same time, molecular dipole moments increase as well, as shown in Fig. 1-b and in Table S1 of the Supporting Information (SI), and those aspects contribute to each other. When ethanol is solvated in aqueous environment and subjected to the external electrostatic gradient, its OH hydrophilic heads re-orient along the field direction more easily than they do in anhydrous ethanol samples, as shown by a direct comparison of Fig. 1-a with Fig. 1-c. This finding may appear somehow counter-intuitive if one considers that, in a 50:50 ethanol-water mixture, a higher percolation degree of H-bonds characterizes the inter-molecular interactions than in pure ethanol. As it occurs in other aqueous mixtures[56], the presence of water molecules increases the overall ethanol dipole moments. In addition, these last rapidly increase upon field exposure, as shown in Fig. 1-d and in Table S1 of the SI, leading thus to a progressively stronger electrostatic coupling with the external field which, in turn, amplifies the OH vector alignment with the field direction, the dipole moment itself, and the dipole fluctuations (notice the curve broadening in Figs. 1-b/d and the standard deviations in Table S1 of the SI). These last are ultimately responsible for the catalysis of the molecular dissociations[35].

Under those conditions, such systems become indeed very reactive. Similarly to the case of neat water[29,39,40], a field strength of 0.25 V/Å is sufficient to trigger the release of hydronium (H_3O^+) and hydroxide (OH^-) ions in an ethanol aqueous solution. The presence of such ions triggers, in turn, the formation of ethanol counter-ions. In fact, at the same field threshold also ethanol cations ($CH_3CH_2OH_2^+$) and anions ($CH_3CH_2O^-$) are detected in the aqueous sample, accordingly to the reaction $2CH_3CH_2OH \rightarrow CH_3CH_2OH_2^+ + CH_3CH_2O^-$. Instead, only starting from a field intensity of 0.30 V/Å the first ethanol counter-ions are formed in neat ethanol. This finding is entirely ascribable to the fact that dipole fluctuations are responsible for deprotonation[35] and water dipole moments are stronger than ethanol dipole moments.

Once formed, those ions easily recombine. Such a process leads indeed to the final neutralization of the starting ion with the same proton the ion itself released soon before. We shall call those ionic species as *static ions*. On the contrary, starting from the respective dissociation thresholds (0.30 V/Å in anhydrous ethanol and 0.25 V/Å in the ethanol-water mixture) correlated proton transfers along the H-bonds lead to the fast conduction of the protonic charge through Grotthuss-like mechanisms. The "molecular wires" along which protons H^+ are transferred are hereon called *ionic wires*, which rule the physical-chemical behavior of the systems at intense field regimes. In both samples, to an increment of

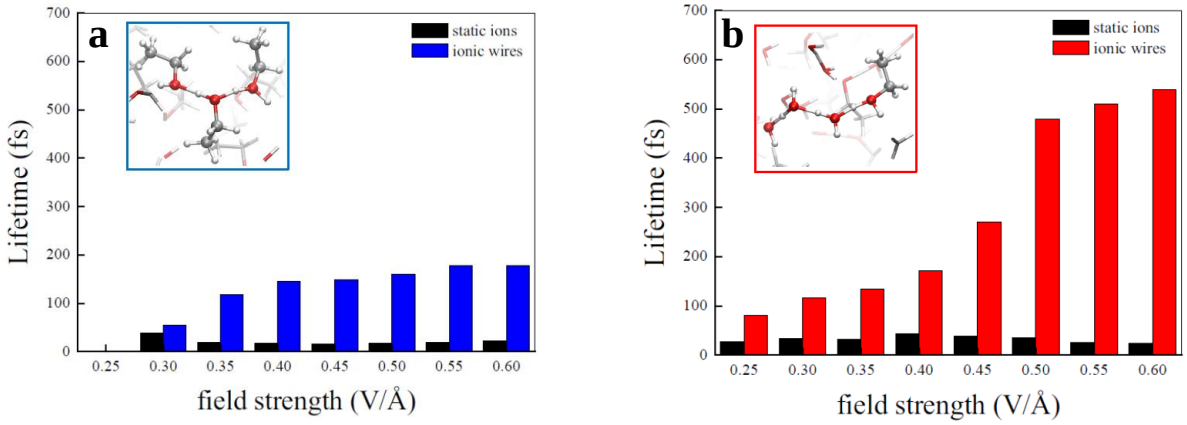

FIG. 2: Histograms of the average lifetimes of the *static ions* and of the *ionic wires* (see text) determined for several field strengths in pure ethanol (a) and in the ethanol-water mixture (b). In the insets, a graphical depiction of the respective *ionic wires* responsible for proton migration.

the field strength corresponds an increase of the average lifetime of the ionic species giving rise to successful proton transfer events (colored histograms). However, whereas in pure

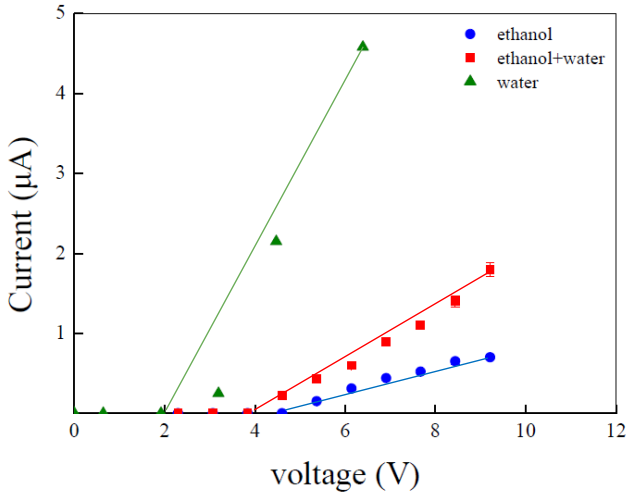

FIG. 3: Ionic current-voltage diagrams of pure ethanol (blue dots), an ethanol aqueous solution (red squares), and neat water (green triangles). Data of pure water stem from Ref.[29]. Points represent the calculated values whereas solid lines are guides for the eye. Ionic conductivities equal to 7.8 mS, 1.3 mS, and 0.5 mS, have been recorded for pure water[29], the ethanol-water mixture, and neat ethanol, respectively.

ethanol (Fig. 2-a) a substantial *plateau* around values of 150 fs is reached starting from 0.40 V/Å, in the ethanol aqueous solution (Fig. 2-b) relatively long-lived *ionic wires*, having lifetimes around 500 fs, are observed at intense field regimes. This means that a sizably more persistent proton transfer activity is present when ethanol is mixed with water. As a consequence, a more conspicuous fraction of ionic species characterizes the ethanol aqueous mixture with respect to the anhydrous case at the maximum field strength explored (*i.e.*, 17% vs. 7%). The field thus stabilizes the transient ionic intermediate species with significantly different efficiency in the two samples, as also highlighted by the respective ionic current-voltage diagrams shown in Fig. 3.

Once the counter-ions are formed in both samples, an additional contribution to the external field is present. The intensity of the local electric fields – due to the ions – can be indeed of the order of 1 V/Å[57–61], which further increases the overall molecular reactivity. In fact, in the ethanol-water mixture we do observe that a field strength of 0.55 V/Å is able to break some C-O covalent bonds and to lead to the synthesis of ethylene ($(CH_2)_2$), as shown in Fig. S5 of the SI and as nominally described by the de-hydration reaction $CH_3CH_2OH \rightarrow (CH_2)_2 + H_2O$. Moreover, also diethyl ether ($CH_3CH_2OCH_2CH_3$) has been detected at the same field strength in both samples. In conjunction with recent results[62,63], these findings suggest that a common feature of the application of intense static electric

fields on alcohols is to trigger de-hydration reactions.

Another reaction channel, not observed in the aqueous mixture, governs the field-induced chemistry of neat ethanol: de-hydrogenation, which leads to the hydrogen (H_2) and acetaldehyde (CH_3CHO) synthesis. As schematically shown in the following chemical transformation:

$$\begin{aligned} 2CH_3CH_2OH &\xrightarrow{0.30\ V/A} CH_3CH_2OH_2^+ + CH_3CH_2O^- \\ &\xrightarrow{0.55\ V/A} H_2 + CH_3CHO + CH_3CH_2OH\,, \end{aligned} \tag{1}$$

and as depicted in Fig. 4, a key role is originally played by the ethanol counter-ions. In Fig. 4-a, the cation should rotate in order to transfer its own excess proton to the nearby anion along the field direction. However, the instantaneous closeness of the methylene groups and the peculiar opposite orientation of the molecular skeletons (Fig. 4-a) open an alternative chemical route for the neutralization process. Such a local and instantaneous frustrated topological arrangement of the counter-ions, in presence of the electrostatic gradient imposed by the field, leads to a distortion of the electron densities. As shown in Fig. 4-b, one of the Wannier centres[64] (*i.e.*, the electron pair) of the methylene group of the ethanol anion shifts toward the hydrogen which is closest to the nearby cation. In a few decades of *fs*, the electron pair that represented a C-H covalent bond, is entirely localized on the hydrogen, forming thus an hydride H^- (Fig. 4-c). Simultaneously, the excess proton H^+ of the nearby ethanol cation is released (Fig. 4-c). This way, the hydride (stemming from the anion) and the proton (stemming from the cation) recombine, leading to the formation of hydrogen, acetaldehyde, and an ethanol molecule (Fig. 4-d). The field-induced reaction products and their yields are reported in Table 1 both for pure ethanol and for the ethanol aqueous mixture.

The formation of hydrogen in anhydrous ethanol is the result of the lack of intermolecular linkages capable to efficiently transfer protonic defects. Under the influence of the external field, such a topological frustration leads to a novel chemical recombination culminating with the H_2 synthesis. Instead, this reaction is unlikely in an ethanol-water mixture, where an higher H-bond percolation degree shapes the intermolecular interactions. The presence of water allows for more flexible ethanol molecular arrangements that are able to react to the field action by maintaining an highly structured H-bond network even in presence of highly oriented molecular configurations. In fact, not only an improved persistence of the molecular wires responsible for proton conduction further dissipates the energetic contribution carried by the field but also the formation of ethylene, depicted in Fig. S5 of the SI, takes place

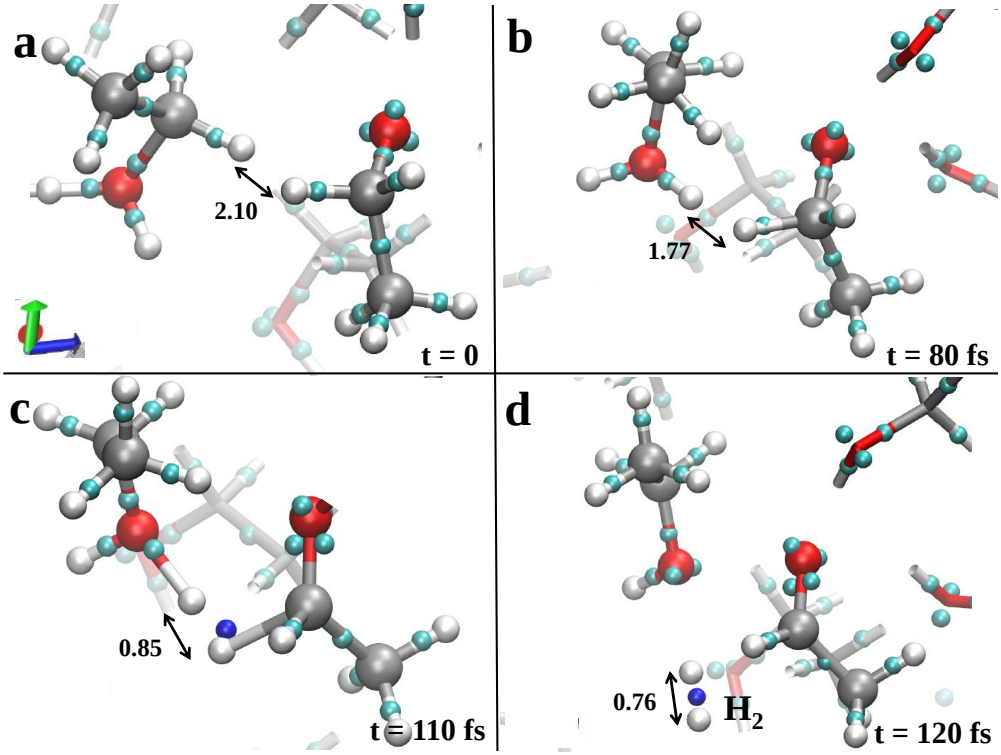

FIG. 4: Hydrogen formation mechanism from liquid ethanol in presence of a static electric field oriented along the positive z-axis (*i.e.*, blue Cartesian axis direction) with strength of 0.55 V/Å. Red, silver, and white coloring refers to oxygen, carbon, and hydrogen atoms, respectively, whereas small cyan spheres represent the Wannier charge centres. The small dark blue sphere in (c) and (d) highlights the electron pair forming H_2. Some distances (in Å) are displayed.

Molecular species (%)	**Ethanol**	**Ethanol+Water**
Diethyl ether	3	4
Ethylene	0	12
Water	3	17
Acetaldehyde	9	0
Hydrogen	9	0

TABLE I: Percent fractions of the molecular species present in the systems at the end of the respective simulations. The fractions are determined as the ratio between the number of molecules of a given species and the total number of ethanol molecules composing the original samples. In the case of the ethanol aqueous mixture, the water content is exclusively referred to the newly synthesized molecules.

through an H-bonded wire of species. It has to be noticed that all the field-induced chemical reactions – including the hydrogen formation – are not very different from the electrochemical reforming of short alcohols. However, all of them are obtained in complete abscence of

chemical catalysts (such as, *e.g.*, sulphuric acid) or surface (such as, *e.g.*, Pt-based or Au-based) catalysts and at room temperature. In fact, as also shown in Fig. S1 of the SI, hydrogen synthesis has been achieved only in samples containing uniquely neat liquid ethanol at an average temperature of 300 K. Besides, the chemical pathway undertaken by the system during such a novel synthesis is completely different from the chemistry typically taking place under plasma conditions, in that all the presented reactions occur keeping the electronic subsystem in its ground-state, as usual in standard AIMD simulations.

As far as the robustness of the employed techniques is concerned, it is worth to stress that equivalent simulations (*i.e.*, exploiting Car-Parrinello molecular dynamics along with the Modern Theory of Polarization and Berry's phases) have been able to predict the molecular dissociation threshold of water under the effect of strong electric fields[29] and to reproduce the Miller experiment[30]. In the latter case, as an example, the fact that field strengths of 0.50 V/Å have been necessary to mimic the well-known Miller syntheses through *ab initio* simulations[30] indicates that such numerical experiments - occurring on a picoseconds time-scale - properly mimic the experimental behavior occurring on longer time-scales.

IV. CONCLUSIONS

In conclusion, we have demonstrated the possibility to synthesize hydrogen from liquid ethanol by means of intense electric fields at room temperature and in absence of any catalyst or template. By atomistically and electronically tracing the behavior of such a system under the field influence, we suggest that peculiar molecular arrangements are directly responsible for the H_2 production. In fact, we have observed that ethanol-water mixtures – where frustrated arrangements of the ethanol counter-ions are unlikely because of a more percolated H-bond network – are not able to synthesize hydrogen under the same circumstances. In other words, whereas an ethanol aqueous solution under intense electric fields is able to maximize its entropy by sustaining an efficient protonic conduction through correlated proton transfers along a diffuse H-bond network, anhydrous ethanol – where intermolecular synergism is sizably less pronounced – maximizes its entropy by creating hydrogen molecules. By following the details here disclosed, the H_2 synthesis could be afforded in catalyst-free experimental setups by means of field emitter tips, where even stronger local field intensities than those here employed are commonly recorded (please see Ref.[27] and references therein).

This study paves the way not only to a new branch of experimental studies on the synthesis of H_2 from clean and sustainable resources, but also toward a more imminent de-carbonized future.

ASSOCIATED CONTENT

A Supporting Information (SI) file is available. Additional results stemming from the *ab initio* molecular dynamics simulations involving *inter alia* the radial distribution functions and the ethylene synthesis reaction mechanism; Electric field considerations and self-consistent field calculations; Transition state detection of the hydrogen synthesis: Committor Analysis; Wannier centres evaluation.

ACKNOWLEDGEMENTS

G. C. thanks F. Saija, A. M. Saitta, and P. V. Giaquinta for useful discussions and initial encouragements.

REFERENCES

[1] Miri, M. J.; Bailey, A. V.; Takacs, G. A. *Introduction to Hydrogen Technology* (John Wiley & Sons, Inc., 2008).

[2] Häussinger, P.; Lohmüller, R.; Watson, A. M. *Ullman's Encyclopedia of Industrial Chemistry* (2011).

[3] Erisman, J. W.; Sutton, M. A.; Galloway, J.; Klimont, Z.; Winiwarter, W. How a Century of Ammonia Synthesis Changed the World. *Nat. Geo.* **2008**, 1, 636-639.

[4] Grochala, W. First Was Hydrogen. *Nat. Chem.* **2015**, 7, 264.

[5] Jacobson, M. Z.; Colella, W. G.; Golden, D. M. Cleaning the Air and Improving Health with Hydrogen Fuel-Cell Vehicles. *Science* **2005**, 308, 1901-1905.

[6] Haile, S. M.; Boysen, D.A.; Chisholm, C. R. I.; Merle, R. M. Solid Acids as Fuel Cell Electrolytes. *Nature* **2001**, 410, 910-913.

[7] Haryanto, A.; Fernando, S.; Murali, S.; Adhikari, S. Current Status of Hydrogen Production Techniques by Steam Reforming of Ethanol: a Review. *Energy Fuels* **2005**, 19, 2098-2106.

[8] Oxtoby, D. W.; Gillis, H. P.; Campion, A.; Helal, H. H.; Gaither, K. P. *Priciples of Modern Chemistry* (5th ed., Thomson Brooks/Cole, 2002).

[9] Walter, M. G.; Warren, E. L.; McKone, J. R.; Boettcher, S. W.; Mi, Q.; Santori, E. A.; Lewis, N. S. Solar Water Splitting Cells. *Chem. Rev.* **2010**, 110, 6446-6473.

[10] Cook, T. R.; Dogutan, D. K.; Reece, S. Y.; Surendranath, Y.; Teets, T. S.; Nocera, D. G. Solar Energy Supply and Storage for the Legacy and Nonlegacy Worlds. *Chem. Rev.* **2010**, 110, 6474-6502.

[11] Fujishima, A.; Honda, K. Electrochemical Photolysis of Water at a Semiconductor Electrode. *Nature* **1972**, 238, 37-38.

[12] Bard, J. A.; Fox, M. A. Artificial Photosynthesis: Solar Splitting of Water to Hydrogen and Oxygen. *Acc. Chem. Res.* **1995**, 28, 141-145.

[13] Kato, H.; Kudo, A. Visible-Light-Response and Photocatalytic Activities of TiO_2 and $SrTiO_3$ Photocatalysts Codoped with Antimony and Chromium. *J. Phys. Chem. B* **2002**, 106, 5029-5034.

[14] Sayama, K.; Mukasa, K.; Abe, R.; Abe, Y.; Arakawa, H. Stoichiometric Water Splitting into H_2 and O_2 Using a Mixture of Two Different Photocatalysts and an IO_3^-/I^- Shuttle Redox Mediator Under Visible Light Irradiation. *Chem. Commun.* **2001**, 1, 2416-2417.

[15] Lu, D.; Takata, T.; Saito, N.; Inoue, Y.; Domen, K. Photocatalyst Releasing Hydrogen from Water. *Nature* **2006**, 440, 295.

[16] Shi, X.; Choi, I. Y.; Zhang, K.; Kwon, J.; Kim, D. Y.; Lee, J. K.; Oh, S. H.; Kim, J. K.; Park, J. H. Efficient Photoelectrochemical Hydrogen Production from Bismuth Vanadate-Decorated Tungsten Trioxide Helix Nanostructures. *Nat. Commun.* **2014**, 5, 4775.

[17] Wang, X.; Maeda, K.; Thomas, A.; Takanabe, K.; Xin, G.; Carlsson, J. M.; Domen, K.; Antonietti, M. A Metal-Free Polymeric Photocatalyst for Hydrogen Production From Water Under Visible Light. *Nat. Mat.* **2009**, 8, 76-80.

[18] Jordan, P. C.; Patterson, D. P.; Saboda, K. N.; Edwards, E. J.; Miettinen, H. M.; Basu, G.; Thielges, M. C.; Douglas, T. Self-Assembling Biomolecular Catalysts for Hydrogen Production. *Nat. Chem.* **2016**, 8, 179-185.

[19] Pawar, G. S.; Tahir, A. A. Unbiased Spontaneous Solar Fuel Production Using Stable $LaFeO_3$ Photoelectrode. *Sci. Rep.* **2018**, 8, 3501.

[20] Mattos, L. V.; Jacobs, G.; Davis, B. H.; Noronha, F. B. Production of Hydrogen From Ethanol: Review of Reaction Mechanism and Catalyst Deactivation. *Chem. Rev.* **2012**, 112, 4094-4123.

[21] Murdoch, M.; Waterhouse, G. I. N.; Nadeem, M. A.; Metson, J. B.; Keane, M. A.; Howe, R. F.; Llorca, J.; Idriss, H. The Effect of Gold Loading and Particle Size on Photocatalytic Hydrogen Production From Ethanol Over Au/TiO_2 Nanoparticles. *Nat. Chem.* **2011**, 3, 489-492.

[22] Gorin, C. F.; Beh, E. S.; Bui, Q. M.; Dick, G. R.; Kanan, M. W. Interfacial Electric Field Effects on a Carbene Reaction Catalyzed by Rh Porphyrins. *J. Am. Chem. Soc.* **2013**, 135, 11257-11265.

[23] Akamatsu, M.; Sakai, N.; Matile, S. Electric-Field-Assisted Anionπ Catalysis. *J. Am. Chem. Soc.* **2017**, 139, 6558-6561.

[24] Yue, L.; Wang, N.; Zhou, S.; Sun, X.; Schlangen, M.; Schwarz, H. The Electric Field as a "Smart" Ligand in Controlling the Thermal Activation of Methane and Molecular Hydrogen. *Angew. Chem. Int. Ed. Engl.* **2018**, 57, 14635-14639.

[25] Aragones, A. C.; Haworth, N. L.; Darwish, N.; Ciampi, S.; Bloomfield, N. J.; Wallace G. G.; Diez-Perez, I; Coote, M. L. Electrostatic Catalysis of a Diels-Alder Reaction. *Nature* **2016**,

531, 88-91.

[26] Shaik, S.; Mandal, D.; Ramanan, R. Oriented Electric Fields as Future Smart Reagents in Chemistry. *Nat. Chem.* **2016**, 8, 1091-1098.

[27] Che, F.; Gray, J. T.; Ha, S.; Kruse, N.; Scott, S. L.; McEwen, J.-S. Elucidating the Roles of Electric Fields in Catalysis: A Perspective. *ACS Catal.* **2018**, 8, 5153-5174.

[28] Balke, N.; Jesse, S.; Carmichael, B.; Okatan, M. B.; Kravchenko, I. I.; Kalinin, S. V.; Tselev, A. Quantification of In-Contact Probe-Sample Electrostatic Forces with Dynamic Atomic Force Microscopy. *Nanotechnology* **2017**, 28, 065704.

[29] Saitta, A. M.; Saija, F.; Giaquinta, P. V. Ab Initio Molecular Dynamics Study of Dissociation of Water Under an Electric Field. *Phys. Rev. Lett.* **2012**, 108, 207801.

[30] Saitta, A. M.; Saija, F. Miller Experiments in Atomistic Computer Simulations. *Proc. Natl. Acad. Sci. USA* **2014**, 111, 13768-13773.

[31] English, N. J.; Waldron, C. J. Perspectives on External Electric Fields in Molecular Simulation: Progress, Prospects and Challenges. *Phys. Chem. Chem. Phys.* **2015**, 17, 12407-12440.

[32] Shaik, S.; de Visser, S. P.; Kumar, D. External Electric Field Will Control the Selectivity of Enzymatic-Like Bond Activations. *J. Am. Chem. Soc.* **2004**, 126, 11746-11749.

[33] Meir, R.; Chen H.; Lai, W.; Shaik, S. Oriented Electric Fields Accelerate Diels-Alder Reactions and Control the Endo/Exo Selectivity. *ChemPhysChem.* **2010**, 11, 301-310.

[34] Wang, Z.; Danovich, D.; Ramanan, R.; Shaik, S. Oriented-External Electric Fields Create Absolute Enantioselectivity in DielsAlder Reactions: Importance of the Molecular Dipole Moment. *J. Am. Chem. Soc.* **2018**, 140, 13350-13359.

[35] Geissler, P. L.; Dellago, C.; Chandler, D.; Hutter, J.; Parrinello, M. Autoionization in Liquid Water. *Science* **2001**, 291, 2121-2124.

[36] King-Smith, R. D.; Vanderbilt, D. Theory of Polarization of Crystalline Solids. *Phys. Rev. B.* **1993**, 47, 1651-1654.

[37] Resta, R. Macroscopic Polarization in Crystalline Dielectrics: the Geometric Phase Approach. *Rev. Mod. Phys.* **1994**, 66, 899-915.

[38] Umari, P.; Pasquarello, A. Ab Initio Molecular Dynamics in a Finite Homogeneous Electric Field. *Phys. Rev. Lett.* **2002**, 89, 157602.

[39] Stuve, E. M. Ionization of Water in Interfacial Electric Fields: an Electrochemical View. *Chem. Phys. Lett.* **2012**, 519-520, 1-17.

[40] Hammadi, Z.; Descoins, M.; Salançon E.; Morin, R. Proton and Light Ion Nanobeams From Field Ionization of Water. *Appl. Phys. Lett.* **2012**, 101, 243110.

[41] Lee, W. K.; Tsoi, S.; Whitener, K. E.; Stine, R.; Robinson, J. T.; Tobin, J. S.; Weerasinghe, A.; Sheehan, P. E.; Lyuksyutov, S. F. Robust Reduction of Graphene Fluoride Using an Electrostatically Biased Scanning Probe. *Nano Res.* **2013**, 6, 767-774.

[42] Miller, S. L. Production of Amino Acids Under Possible Primitive Earth Conditions. *Science* **1953**, 117, 3046.

[43] Giannozzi P.; Baroni, S.; Bonini, N.; Calandra, M.; Car, R.; Cavazzoni, C.; Ceresoli, D.; Chiarotti, G. L.; Cococcioni, M.; Dabo, I.; Dal Corso, A.; de Gironcoli, S.; Fabris, S.; Fratesi, G.; Gebauer, R.; Gerstmann, U.; Gougoussis, C.; Kokalj, A.; Lazzeri, M.; Martin-Samos, L.; Marzari, N.; Mauri, F.; Mazzarello, R.; Paolini, S.; Pasquarello, A.; Paulatto, L.; Sbraccia, C.; Scandolo, S.; Sclauzero, G.; Seitsonen, A. P.; Smogunov, A.; Umari, P.; Wentzcovitch, R. M. QUANTUM ESPRESSO: a Modular and Open-Source Software Project for Quantum Simulations of Materials. *J. Phys.: Condens. Matter* **2009**, 21, 395502-395537.

[44] Car, R.; Parrinello, M. Unified Approach for Molecular Dynamics and Density-Functional Theory. *Phys. Rev. Lett.* **1985**, 55, 2471.

[45] Berry, M. V. Quantal Phase Factors Accompanying Adiabatic Changes. *Proc. R. Soc. Lond. A* **1984**, 392, 45.

[46] Nunes, R. W.; Vanderbilt, D. Real-Space Approach to Calculation of Electric Polarization and Dielectric Constants. *Phys. Rev. Lett.* **1994**, 73, 712.

[47] Nunes, R. W.; Gonze, X. Berry-phase Treatment of the Homogeneous Electric Field Perturbation in Insulators. *Phys. Rev. B* **2001**, 63, 155107.

[48] Resta R. Quantum-Mechanical Position Operator in Extended Systems. *Phys. Rev. Lett.* **1998**, 80, 1800.

[49] Gonze, X.; Ghosez, Ph.; Godby, R.W. Density-Polarization Functional Theory of the Response of a Periodic Insulating Solid to an Electric Field. *Phys. Rev. Lett.* **1995**, 74, 4035.

[50] Gonze, X.; Ghosez, Ph.; Godby, R.W. Density-Functional Theory of Polar Insulators. *Phys. Rev. Lett.* **1997**, 78, 294.

[51] Rappe, A. M.; Rabe, K. M.; Kaxiras, E.; Joannopoulos, J. D. Optimized Pseudopotentials. *Phys. Rev. B* **1990**, 44, 13175.

[52] Perdew, J. P.; Burke, K.; Ernzerhof, M. Generalized Gradient Approximation Made Simple. *Phys. Rev. Lett.* **1996**, 77, 3865 and *Phys. Rev. Lett.* **1997**, 78, 1396.

[53] Grimme, S.; Antony, J.; Ehrlich, S.; Krieg, H. A Consistent and Accurate Ab Initio Parametrization of Density Functional Dispersion Correction (DFT-D) for the 94 Elements H-Pu. *J. Chem. Phys.* **2010**, 132, 154104.

[54] Marsalek, O.; Markland, T. E. Quantum Dynamics and Spectroscopy of Ab Initio Liquid Water: The Interplay of Nuclear and Electronic Quantum Effects. *J. Phys. Chem. Lett.* **2017**, 8, 1545-1551.

[55] Sekine, Y.; Haraguchi, M.; Tomioka, M.; Matsukata, M.; Kikuchi, E. Low-Temperature Hydrogen Production by Highly Efficient Catalytic System Assisted by an Electric Field. *J. Phys. Chem. A* **2010**, 114, 3824-3833.

[56] Cassone, G.; Sponer, J.; Sponer, J. E.; Pietrucci, F.; Saitta, A. M.; Saija, F. Synthesis of (D)-erythrose From Glycolaldehyde Aqueous Solutions Under Electric Field. *Chem. Commun.* **2018**, 54, 3211-3214.

[57] Sellner, B.; Valiev, M.; Kathman, S. M. Charge and Electric Field Fluctuations in Aqueous NaCl Electrolytes. *J. Phys. Chem. B* **2013**, 117, 10869-10882.

[58] Reischl, B.; Köfinger, J.; Dellago, C. The Statistics of Electric Field Fluctuations in Liquid Water. *Mol. Phys.* **2009**, 107, 495-502.

[59] Bronstein, Y.; Depondt, P.; Bove, L. E.; Gaal, R.; Saitta, A. M.; Finocchi, F. Quantum Versus Classical Protons in Pure and Salty Ice Under Pressure. *Phys. Rev. B* **2016**, 93, 024104.

[60] Cassone, G.; Calogero, G.; Sponer, J; Sponer, J.; Saija, F. Mobilities of Iodide Anions in Aqueous Solutions for Applications in Natural Dye-Sensitized Solar Cells. *Phys. Chem. Chem. Phys.* **2017**, 20, 13038-13046.

[61] Cassone, G.; Creazzo, F.; Giaquinta, P. V.; Sponer, J.; Saija, F. Ionic Diffusion and Proton Transfer in Aqueous Solutions of Alkali Metal Salts. *Phys. Chem. Chem. Phys.* **2017**, 19, 20420-20429.

[62] Cassone, G.; Pietrucci, F.; Saija, F.; Guyot, F.; Saitta, A. M. One-step Electric-Field Driven Methane and Formaldehyde Synthesis From Liquid Methanol. *Chem. Sci.* **2017**, 8, 2329-2336.

[63] Cassone, G.; Pietrucci, F.; Saija, F.; Guyot, F.; Sponer, J.; Sponer, J. E.; Saitta, A. M. Novel Electrochemical Route to Cleaner Fuel Dimethyl Ether. *Sci. Rep.* **2017**, 7, 6901.

[64] Marzari, N.; Mostofi, A. A.; Yates, J. R.; Souza, I.; Vanderbilt, D. Maximally Localized Wannier Functions: Theory and Applications. *Rev. Mod. Phys.* **2012**, 84, 1419-1475.

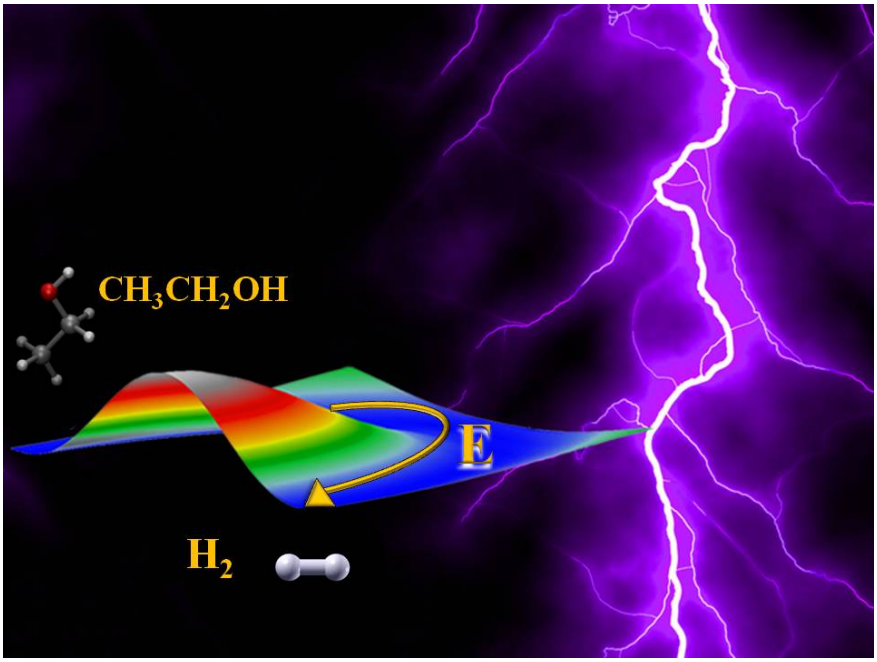

TOC Graphic